Collective Pitch Control of Wind Turbines using Stochastic Disturbance Accommodating Control

Irving P. Girsang* and Jaspreet S. Dhupia
Graduate Student, Assistant Professor, School of Mechanical and Aerospace Engineering, Nanyang Technological University, Singapore Email: irving1@e.ntu.edu.sg, djaspreet@ntu.edu.sg

Received February 15, 2013; Accepted July 2, 2013

Fidelity of a plant's dynamic model is a concern in any controller design process. In this context, fidelity refers to which dynamics of the plant needs to be included in the control model and which dynamics can be left out or approximated. Studies on wind turbine control have shown that modelling error due to the unmodeled dynamics can lead to unstable closed-loop dynamics. This paper investigates the use of Kalman estimator to design the Stochastic Disturbance Accommodating Control (SDAC) scheme to stabilize the system in the presence of the unmodeled dynamics. Performance of the presented control scheme is investigated through simulations on two different wind turbine configurations under turbulent wind conditions with different mean wind speeds and turbulence intensities using FAST (Fatigue, Aerodynamics, Structures, and Turbulence) aero-elastic tool. The generator speed regulation, drivetrain load, and control effort of the presented control scheme are compared with those of the baseline Gain Scheduled Proportional Integral (GSPI) controller. The results indicate better speed regulation and lower drivetrain load for the presented SDAC under the tested wind conditions.

1. INTRODUCTION

The interest in renewable energies, of which wind energy is among the most important ones, is increasing in the recent decades. Horizontal axis wind turbines have become the most common wind energy conversion systems and are expected to compete with fossil fuel power plants in the near future. To do so, it requires better technology to reduce the cost of power generation and innovative control strategies can play an essential part in this context. Control methods can decrease the cost of wind energy by keeping the turbine operating close to its maximum efficiency and preserving the effective lifetime of the turbine by reducing the structural loads. The popular variable speed variable pitch capabilities on modern utility scale turbines are further promoting the development of novel controllers to accomplish these objectives.

A variable speed variable pitch wind turbine operates in five major operating regions, as shown in Fig. 1. It depicts the output power of the wind turbine generator as a function of the effective wind speed. Region 1 lies below the cut-in wind speed. In this region, the mean power available in the wind is insufficient to overcome the electrical and mechanical losses. Region 2 lies between the cut-in and rated wind speeds. In this region, the turbine operates to capture as

*Corresponding author: Irving P. Girsang, Email: irving1@e.ntu.edu.sg

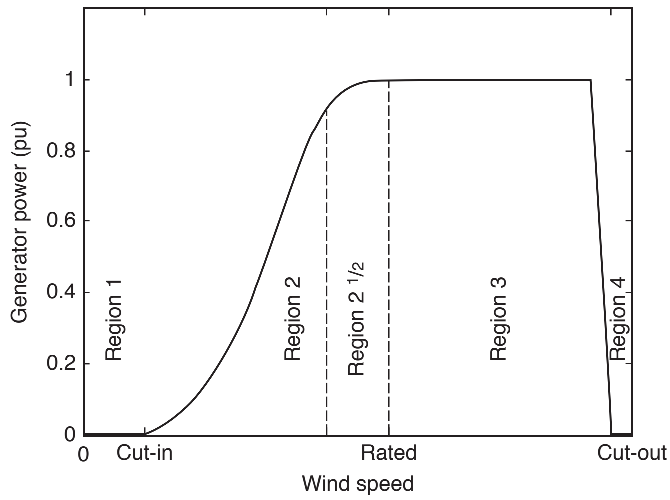

Figure 1: Typical power curve of variable speed variable pitch wind turbine, 1 pu (per unit) power = rated power of the generator.

much wind energy as possible by utilizing the power electronics to control the generator torque. Region $2\frac{1}{2}$ starts close to the rated wind speed and helps to smoothen the transition between Regions 2 and 3. Region 3, which is considered in this paper, lies between the rated and cut-out wind speeds. In this region, the turbine operates to produce constant power output at its rated value. This constant rated power can be achieved by operating the turbine at the constant generator torque and regulating a constant generator speed through the feedback control, wherein pitching of the blades acts as the control actuation. Finally, Region 4, lies above the cut-out wind speed. In this region, the turbine is parked to prevent damages to the wind turbine structure due to enormous loads coming from extremely high wind speed.

The predominant methods of regulating constant generator speed in Region 3 are based on the control methods utilizing collective blade pitch actuation. The controller types commonly implemented by industries are the model-based Proportional-Integral-Derivative (PID) controller [1, 2]. The Disturbance Accommodating Control (DAC), which was first introduced by Johnson [3, 4], has emerged into the wind turbine applications in the last decade. For Region 3, the DAC regards the oncoming wind as a persistent disturbance input to the plant. Numerical simulations and field tests have successfully demonstrated the capability of DAC to attenuate the effects of the changing wind speed [5–11]. However, as reported in [5], this approach is sensitive to modeling errors. Simulations on DAC that is designed based on a lower order model (assuming only the torsional flexibility of the drivetrain), but implemented on a turbine with higher order dynamics (having flexibilities at other components, such as blades and towers) result in an unstable system response. Moreover, when measurement noise is present, additional low-pass filter is required to prevent noisy actuation signal that can cause chattering or saturation of the actuator. However, recent study in [12] has shown that the linear estimator based DAC with a low-pass filtered measurement signal leads to degradation of control performance.

This paper presents a new control strategy based on the Stochastic Disturbance Accommodating Control (SDAC) concept [13] for variable pitch, but not necessarily variable speed, wind turbines. The presented control strategy compensates for the unmodeled dynamics (i.e. the neglected modes during the design of the controller), the changing wind speed that acts as the external disturbance, as well as the measurement noise. The term "stochastic" stems from the assumption of a stochastic "true" plant, which has uncertainties due to the unmodeled dynamics and/or modeling errors. These inherent uncertainties can cause instability when only the nominal control feedback law is applied. In order to achieve stability, the proposed approach uses a tuned Kalman estimator in the feedback loop to estimate both plant and disturbance states from a noisy measurement signal. Some additional practical advantages of implementing the Kalman estimator include easy tuning of the estimator parameters (i.e. the noise covariance matrices) and a more economic implementation, as the Kalman estimator can be used directly to filter noisy measurements.

To obtain general conclusions regarding the controller performance, simulations were performed on two different turbine configurations with augmented actuator models, which are introduced in Section 2. The control performance was evaluated on high order turbine models, which were incorporated in FAST (Fatigue, Aerodynamics, Structures, and Turbulence) aeroelastic tool and simulated in the Simulink environment. All the available structural modes of the turbine models were activated, except for the yaw mode. On the other hand, the SDAC was designed without considering the actuator dynamics and solely based on the torsional model of the wind turbine drivetrain. Finally, Section 4 compares the simulated performance of the SDAC in terms of the speed regulation, control cost, and drivetrain load with those of the baseline Gain Scheduled Proportional-Integral (GSPI) controller.

2. WIND TURBINE MODEL

The two turbines considered in this work are the NREL (National Renewable Energy Laboratory) CART (Control Advanced Research Turbine) and the NREL 5-MW Reference Turbine. These two turbines respectively represent the lower and higher ranges of the modern utility scale wind turbines. CART is a turbine currently under operation at the National Wind Technology Centre in Colorado [14]. It is purposely built and operated to facilitate the implementations and testings of various wind turbine control algorithms. The 5-MW Reference Turbine is a virtual turbine created to study various aspects of offshore turbine design and development through numerical simulations [15]. The 5-MW Turbine model can also be utilized assuming an onshore environment, which is implemented in this study. Design parameters of both turbines are contrasted in Table 1.

2.1. Linearized model of wind turbine

Besides performing time marching simulation of a wind turbine structural response, FAST can also be used to create the linearized model of a turbine. For the design of the Stochastic Disturbance Accommodating Control (SDAC) in this paper, only the flexibility of the drivetrain was considered in the control model of each turbine. Other structural parts of the turbines are assumed rigid. Figure 2 shows the drivetrain model, where J_{rot} and J_{gen} are respectively the inertia of the rotor and generator, θ_{rot} and θ_{gen} are respectively the angular position of the rotor

Table 1: Design parameters of CART and NREL 5-MW turbines

Turbine parameters	CART	NREL 5-MW
Power Rating [MW]	0.6	5
Number of Blades	2	3
Generator Rated Speed [RPM]	1,800	1,173.7
Rotor Diameter [m]	43.3	126
Hub Height [m]	36.6	87.6
Pitch Rate Limit [°/s]	18	8

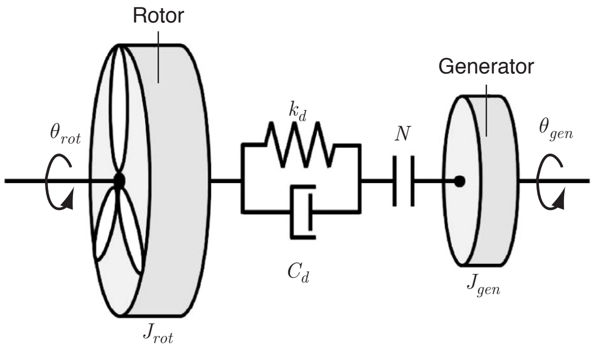

Figure 2: Two-mass model of a wind turbine drivetrain.

and generator. k_d and c_d are respectively the equivalent torsional stiffness and damping of the drivetrain, and N is the overall gear ratio.

The two considered turbine models were linearized around the wind speed of 16 m/s for the CART and 18 m/s for the NREL 5-MW. These wind speeds are located at the middle of the rated and cut-out wind speeds of the turbines. Each of these wind speeds is referred in this paper as the linearization wind speed. The state space formulation of this assumed turbine model can be expressed as:

$$\dot{x}_m = A_m x_m + B_m u_m + B_{d,m} u_{d,m} \tag{1}$$

where

$$x_m = \left\{ \dot{\tilde{\theta}}_{rot} \; \tilde{\theta}_{rot} - \tilde{\theta}_{gen} \; \dot{\tilde{\theta}}_{gen} \right\}^T, \; y_m = \tilde{\beta}, \; u_{d,m} = \tilde{v}_w$$

The three states considered in vector x_m are the perturbed (from equilibrium points) rotor angular velocity, torsional deflection of the drivetrain, and generator angular velocity, respectively. The control input is the perturbed actual pitch angle $\tilde{\beta}$ and the disturbance input is the perturbed wind speed $\tilde{v}_w$. This model is referred as the three-state model in [5].

2.2. Pitch actuator model

Pitch actuators for wind turbines can be either hydraulic or electric motors. The actuator is necessary to alter the pitch angle of a blade in order to regulate the aerodynamic torque generated by the oncoming wind. However, FAST does not provide any models to represent the dynamics of the pitch actuators. Two different actuator models are adopted due to the distinctly different rating and size of the turbines considered herein.

A first order actuator model is adopted to represent the actual electric motor drive installed in CART [16, 17]:

$$\beta = \frac{30}{s+30} \beta_c \tag{2}$$

where β_c is the commanded pitch angle, which acts as the input to the actuator.

A second order actuator model is commonly used to represent the piston servo system commonly installed in megawatt scale turbines [18–21], such as the NREL 5-MW Reference Turbine:

$$\beta = \frac{\omega_n^2}{s^2 + 2\zeta\omega_n + w_n^2}\beta_c \tag{3}$$

Parameters of the second order actuator model were chosen to have similar cut-off frequency (the - 3 dB frequency) to that of CART, with $w_n = 30$ rad/s and $\zeta = 0.7$.

It is important to mention that in this paper, the actuator models are implemented only for the evaluation of the control performance. It is not to be considered during the design of the controller (i.e. during the design stage, it is assumed that $\beta_c = \beta$), due to a reason elaborated in the following section.

3. COLLECTIVE PITCH CONTROL

In order to facilitate a fair comparison, both controllers were designed to have the same number of sensors. Each controller takes the generator speed measurement as its only input and gives the collective pitch command (i.e. equal pitch angle for all blades) as its output.

3.1. Baseline gain scheduled PI control

The Gain Scheduled PI (GSPI) controller was designed as the baseline controller in simulating the response of each turbine (CART: [6] and NREL 5-MW: [22]). In the design of this controller, the wind turbine drivetrain was modelled as a rigid inertia. The turbine structural flexibilities and actuator model were not considered. A low-pass filter is implemented to attenuate the measurement noise and the effects of unmodeled dynamics [6, 12, 22].

In a realistic turbulent wind, the instantaneous wind speed occasionally dips from Region 3 to Region 2 while the Region 3 controller is being implemented. It may stay in Region 2 for a while before returning back to Region 3, which can cause the integral windup issues. Therefore, an integral anti windup is implemented to tackle such problem. The schematic of this baseline control is shown in Fig. 3.

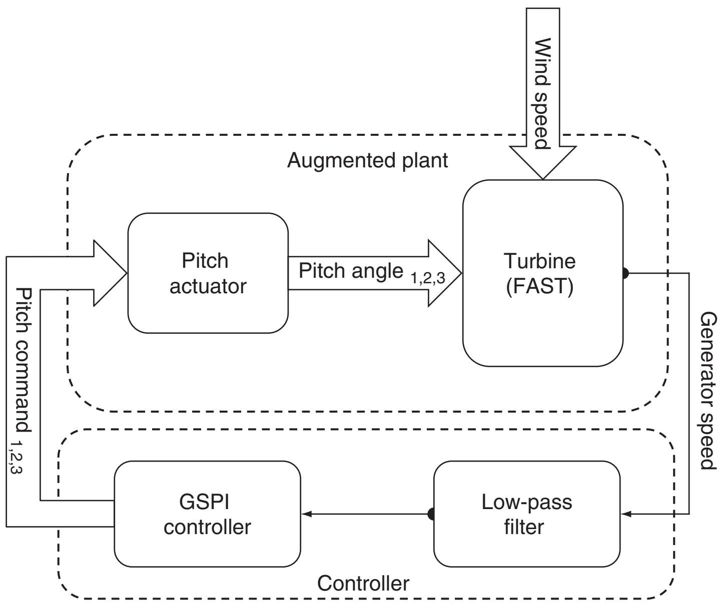

Figure 3: Schematic of gain scheduled PI control (GSPI).

3.2. Stochastic disturbance accommodating control

The Stochastic Disturbance Accommodating Control (SDAC) scheme is designed based on the linearized plant model in eqn (1). For both turbines, (A_m, B_m) is controllable. Thus, a feedback control law with static gain matrix can be designed as the nominal control law in order to place the poles of the closed-loop system at the desired locations:

$$\bar{u}_m = -G_m x_m \tag{4}$$

In the design of the SDAC for wind turbine application, the wind disturbance can be modelled as a persistent disturbance [3] and the effects of unmodeled dynamics can be assumed to introduce a Gaussian white process noise into the system. This results in a disturbance dynamics that is modeled as:

$$\dot{x}_{d,m} = A_d x_{d,m} + \mathcal{W} \tag{5}$$

$$u_{d,m} = C_d x_{d,m} \tag{6}$$

where $\mathcal{W}$ is the zero mean Gaussian white process noise due to the unmodeled dynamics. In this paper, the change in wind speed is assumed to be a step persistent disturbance, which has been shown to be an adequate approximation of the uniform wind speed [5-7], with $A_d = 0$ and $C_d = 1$.

To attenuate the effect of the disturbance input $u_{d,m}$ on the system dynamics, one can theoretically set an additional feedback control law based on eqns (1, 5, 6):

$$u_m^* = -G_{d,m} x_{d,m} \tag{7}$$

where, for $C_d = 1$

$$G_{d,m} = \left(B_m^T B_m\right)^{-1} B_m^T B_{d,m}$$

Thus, the total control law can be stated as:

$$u_m = \tilde{\beta} = \bar{u}_m + u_m^* = -[G_m \; G_{d,m}] \begin{Bmatrix} x_m \\ x_{d,m} \end{Bmatrix} \tag{8}$$

The actuator model is not considered during the controller design stage because it results in a steady state error in the speed regulation if the controller gains are not carefully tuned, which can be explained as follows.

If the actuator model was considered in controller design, an augmented (i.e. the wind turbine with actuator) plant model would be created, resulting in the following state space representation:

$$\dot{x}_p = A_p x_p + B_p \tilde{\beta}_c + B_{d,p} u_{d,m} \tag{9}$$

$$\begin{Bmatrix} \dot{x}_m \\ \dot{x}_a \end{Bmatrix} = \begin{bmatrix} A_m & B_m \\ 0 & A_a \end{bmatrix} \begin{Bmatrix} x_m \\ x_a \end{Bmatrix} + \begin{bmatrix} 0 \\ B_a \end{bmatrix} \tilde{\beta}_c + \begin{bmatrix} B_{d,m} \\ 0 \end{bmatrix} u_{d,m}$$

where

$$\dot{x}_a = A_a x_a + B_a \tilde{\beta}_c$$

represents the actuator model in the state space representation. Following the previously developed approach for the turbine model, one can set the control law for the augmented plant to be:

$$\tilde{\beta}_c = -[G_p \; G_{d,p}] \begin{Bmatrix} x_p \\ x_{d,m} \end{Bmatrix} \tag{10}$$

so that in the steady state (i.e. for $\dot{x}_p = 0$) the augmented states can be expressed as:

$$x_{p,ss} = (A_p - B_p G_p)^{-1} (B_p G_{d,p} - B_{d,p}) x_{d,m} \tag{11}$$

Using the similar analogy as in eqn (7), a disturbance attenuation for the augmented plant can be achieved by setting the disturbance state gain as $G_{d,p} = (B_p^T B_p)^{-1} B_p^T B_{d,p}$. However, due to the structures of both the control and disturbance input matrices, the resultant gain would always be zero. In other words, there would be no actuation that acts to attenuate the effect of the changing wind speed. Moreover, it implies that for any tuned values of $G_{d,p} \neq 0$, the term $(B_p G_{d,p} - B_{d,p}) \neq 0$.

Physically, one can see that the augmented system in eqn (9) does not relate the augmented system states x_p to aerodynamic effect of the commanded change in the pitch angle $\tilde{\beta}_c$. In the turbine model of eqn (1) this aerodynamic coupling is served by B_m that relates x_m to u_m. As a result, the disturbance state gain computed based on the augmented system model does not give a satisfactory disturbance rejection response.

It is important to note that in steady state, the actuator state x_a of the augmented state x_p in eqn (11) contains the actual perturbed pitch angle $\tilde{\beta}$. This pitch angle must not be zero when regulating the generator speed for the case of non-zero wind disturbance input. However, it is possible to tune the $G_{d,p}$ so that the turbine states x_m have the desired zero steady state values. In doing so, the tuned $G_{d,p}$ is now dependant on the value of G_p. In other words, the feedback gain for the disturbance state is different for different desired closed-loop pole locations. This in turn complicates the tuning process. On the contrary, the disturbance accommodating controller designed by omitting the actuator model does not suffer from any steady state error. This stems from the fact that $\beta = \beta_c$ for common pitch actuators at the steady state. This conforms with the basic assumption used in the derivation of the control feedback law in eqn (8). Therefore, it is recommendable to omit the dynamics of pitch actuator in the design of the SDAC.

As only the generator speed is available from the measurement, it is necessary to design a state estimator, to obtain estimates of the other turbine and disturbance states. The linearized plant model of eqn (1) can be augmented with the disturbance model of eqn (5):

$$\dot{x}_o = A_o x_o + B_o u_m + D_o \mathcal{W} \tag{12}$$

$$\begin{Bmatrix} \dot{x}_m \\ \dot{x}_{d,m} \end{Bmatrix} = \begin{bmatrix} A_m & B_{d,m} \\ 0 & 0 \end{bmatrix} \begin{Bmatrix} x_p \\ x_{d,m} \end{Bmatrix} + \begin{bmatrix} B_m \\ 0 \end{bmatrix} u_m + \begin{bmatrix} 0 \\ I \end{bmatrix} \mathcal{W}$$

and the generator speed measurement can be expressed as:

$$y = C_o x_o + V = [C_m \; 0] \; x_o + \mathcal{V} \tag{13}$$

where $\mathcal{V}$ is zero mean Gaussian white measurement noise.

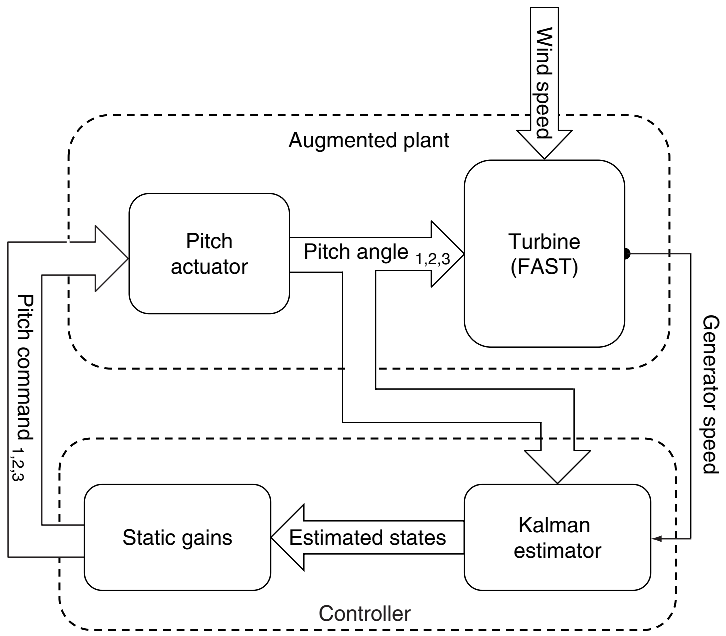

Figure 4: Schematic of stochastic DAC.

For both turbines, (A_o, C_o) is found to be observable. Thus, even though the disturbance state is not measured, based on the assumed stochastic properties of $\mathcal{W}$ and $\mathcal{V}$, an optimal estimator such as a Kalman estimator can be implemented in the feedback loop to estimate the unmeasured system and disturbance states from the noisy measurement. The estimator dynamics can be written as:

$$\dot{\hat{x}}_o = A_o\hat{x}_o + B_o um + K(x_o - \hat{x}_o) + K\mathcal{V} \tag{14}$$

where the Kalman gain can be calculated as $K = PC_o^T R^{-1}$ and the estimation error covariance matrix $P = E[(x_o - x_o)(x_o - x_o)^T]$ can be obtained by solving the continuous-time Riccati equation:

$$\tilde{P} = A_o P + PA^T{}_o - KC_oP + D_oQD^T{}_o \tag{15}$$

where Q and R are the process and measurement noise covariance matrices, respectively. As R can be obtained during the calibration of the measurement sensor, Q acts as the tuning parameter for the Kalman estimator. The schematic of the proposed control scheme is shown in Fig. 4.

4. SIMULATION RESULTS AND DISCUSSIONS

4.1. Simulation with step wind inputs

As a tuning guideline of the proposed SDAC, it is important to note that if $Q = 0$, then $x_{d,m} = 0$. Thus, the total control law in eqn (8) becomes just the nominal control. For the case presented in this study, the nominal control $\bar{u}_m$ that acts on the "true" plant (with higher order dynamics) results in an unstable system. Therefore, selecting too small Q will also result in an unstable system.

Figure 5 shows the generator speed (i.e. output) and commanded pitch angle (i.e. input) responses from the simulation with $Q = 0$ for the NREL 5-MW Reference Turbine. The wind input for this simulation was a constant uniform wind speed of 16 m/s (i.e. the linearization

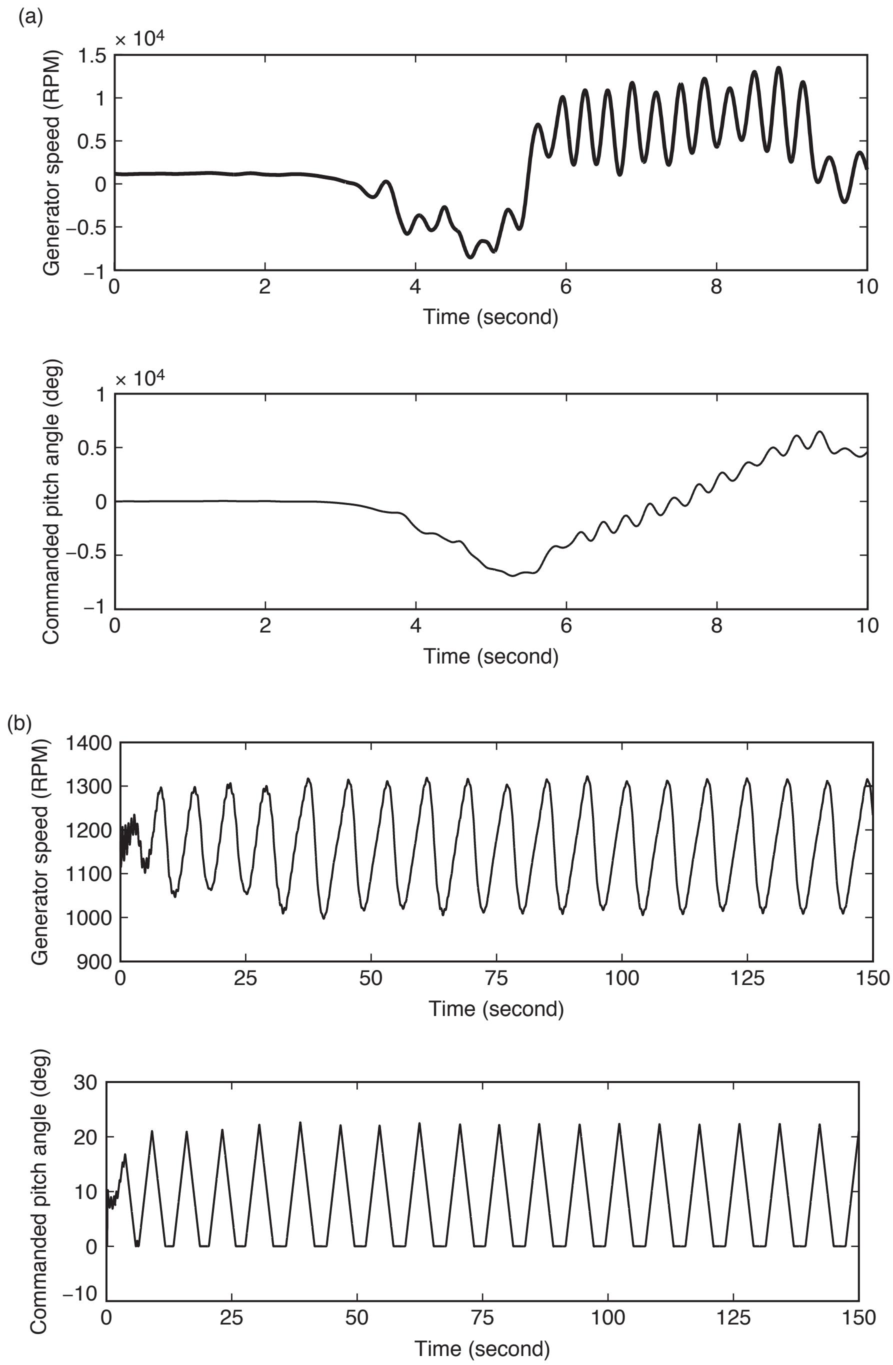

Figure 5: Deterioration in system responses for $Q = 0$ (a) with an ideal (limitless) pitch actuator, (b) with a pitch actuator having saturation limits.

wind speed of this turbine). As discussed in the preceding section, the designed SDAC considers only the dynamics of the wind turbine drivetrain, while the "true" plant (i.e. the FAST turbine model) includes additional structural dynamics of the blades and tower. Despite designing the nominal control law of eqn (4) that has stable closed-loop poles, the responses shows unexpected deterioration of performance due to the additional structural modes (i.e. the unmodeled dynamics), as shown in Fig. 5. Similar performance deterioration was also reported while simulating the performance of the three-state DAC, previously designed in [5]. Figure 5a shows that the deteriorated performance is indeed due to the unmodeled high order dynamic, which in turn forces the saturation of the actuator as illustrated in Fig. 5b.

On the other hand, selecting a large Q will compel the Kalman estimator to completely rely upon the measurement. Therefore, the noise associated with the measurement signal is directly transmitted into the state estimates, and then the control input [13]. In simulating the response of both turbines, a Gaussian white noise with a variance of 10 RPM^2 was added into the measured generator speed signal, giving a signal to noise ratio (SNR) of approximately 50 dB. Figure 6 shows the simulated responses of the NREL 5-MW Reference Turbine with a large diagonal matrix Q and the tuned one. A rough trial-and-error tuning of the diagonal matrix Q was performed to achieve similar generator speed response under step wind speed input with that of the baseline GSPI controller at the linearization wind speed. This is illustrated in Fig. 7 for the NREL 5-MW Reference Turbine. The Q was further fine tuned to have a similar root mean square (RMS) generator speed error at the chosen linearization mean turbulent wind speed, as discussed in the following subsection.

Good estimate of the wind speed is critical because it directly affects the disturbance attenuation. Figure 8 shows the wind estimation of the SDAC with the tuned Q for the NREL 5-MW Reference Turbine under multi-step wind speed input. Being a linear controller, it is expected that the estimation deteriorates as the wind speed deviates away from the linearization wind speed of 16 m/s due to the non-linearity.

4.2. Simulation with turbulent wind inputs

Simulations were performed under turbulent wind conditions to evaluate and compare the performance of the proposed SDAC to that of the baseline GSPI controller. Each of them simulated a 600-second event, as recommended by the IEC 61400-12 standard [23]. This paper assumes solely the Region 3 control objectives. Therefore, no switching of control logic is implemented although the instantaneous wind speed occasionally drops to Region 2 or rises to Region 4 for a while.

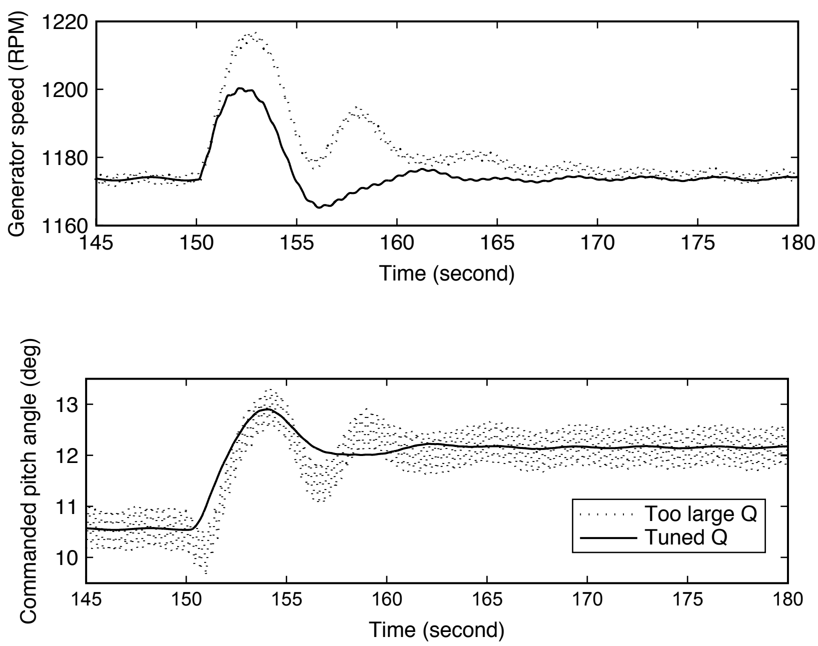

Figure 6: Noisy input and output responses due to large Q.

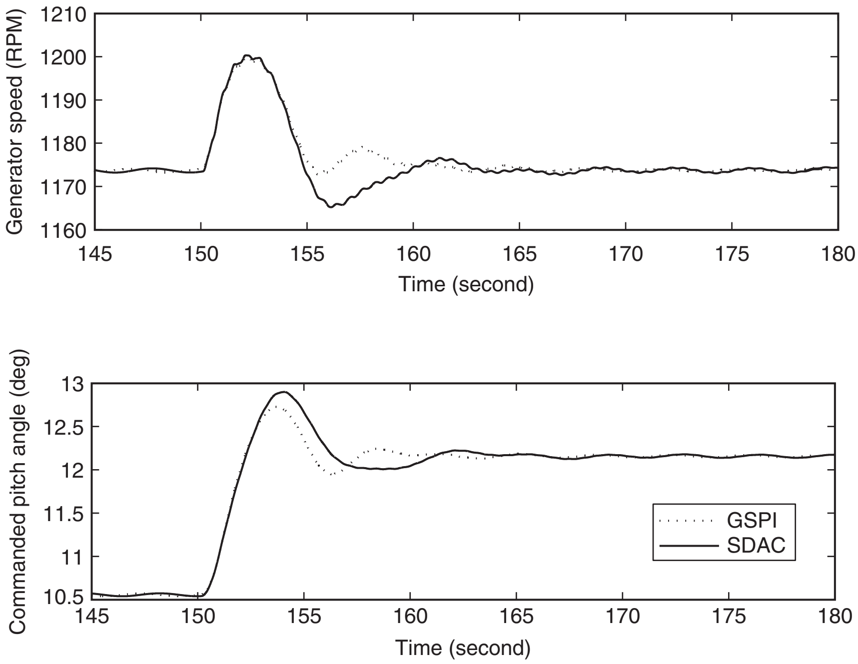

Figure 7: Similar generator speed response GSPI and SDAC after tuning the Q 4.2.1 NREL CART.

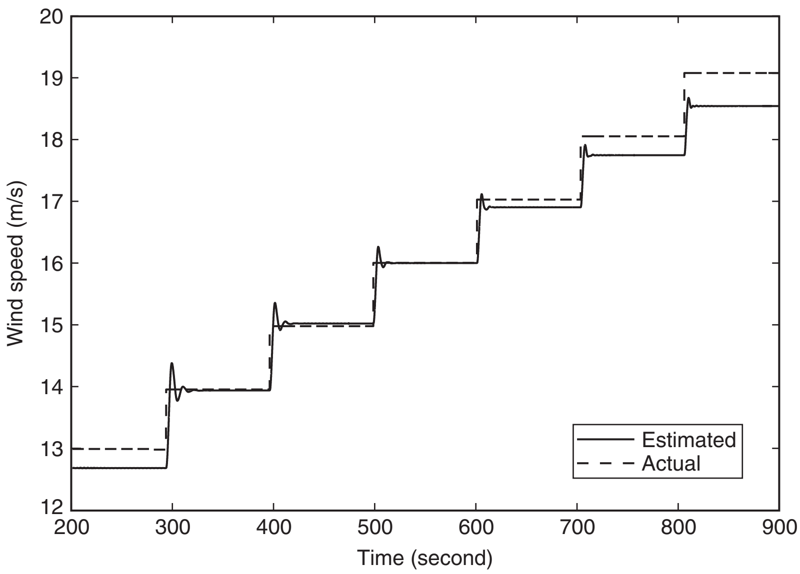

Figure 8: Estimated and actual wind speed of SDAC.

TurbSim was used to generate realistic hub-referenced turbulent wind fields for both turbines following the Kaimal spectrum [24]. Five cases were simulated for each turbine. Nine different turbulence seeds were used for each case, resulting in a total number of 180 simulations. For each turbine, four of the tested cases have different mean wind speed with low turbulence intensity, which is class C of the IEC 61400-1 standard [25]. The remaining case has high turbulence intensity at the linearization mean wind speed. It is class B for the CART and class A for the NREL 5-MW. Simulations on other cases beyond these mean wind speeds and turbulence intensities resulted in an invalid comparison as the integral windup created severe performance deterioration for the baseline GSPI controller, even though the integral anti windup was being implemented.

Relative performance between the controllers is compared in terms of the speed regulation, control cost, and damage equivalent load (DEL) of the drivetrain. The speed regulation is compared using the root mean square (RMS) and maximum value of the speed error from the rated generator speed. The control cost is compared using the RMS of the blade pitch rate. The DEL was computed using the MLife code [26] that takes time series data of the torque transmitted through the low speed shaft (LSS) to the gearbox. The wind turbine gearbox is regarded as the critical component, because its failures are responsible for over 20% of the downtime of wind turbines [27, 28]. Therefore, in evaluating the DEL, the slope of the cyclic stress to cycles-to-failure (i.e. the *SN* curve) is chosen to be 8, which is typical for the wind turbine gears made from case-hardened cast iron.

Notched boxplot for each performance metric is plotted side by side for graphical comparison. The notch feature serves to highlight the difference among the medians of the data groups. Non-overlapping notches offer an evidence of a statistically significant difference between two compared boxplots.

In order to standardize the comparison, both controllers were tuned to achieve similar RMS generator speed error at the reference operating condition. This reference operating condition corresponds to the one at the linearization mean wind speed with lower turbulence intensity. All performance metrics were normalized with respect to the median of the corresponding metric of the reference operating condition.

4.2.1. NREL CART

The speed regulation of the two controllers is compared in term of the RMS generator speed error in Fig. 9a. The two controllers achieved the desired similar performance at the reference operating condition. The maximum generator speed error is compared in Fig. 9b.

In term of the RMS generator speed error, there is a distinct trend between the controllers across the tested mean wind speeds with similar turbulence class. The GSPI controller shows an expected trend in which the best speed regulation is achieved at the linearization mean wind speed of 18 m/s. Having been designed to take into account the nonlinear turbine aerodynamics, the GSPI controller performs much better than a PI controller. Nonetheless, the GSPI controller cannot completely eliminate the performance degradation due to the nonlinearity. On the other hand, having been designed as a linear controller, the SDAC shows a different trend, in which the median and variation of the RMS speed error increases as the mean wind speed decreases. One explanation can be offered through investigation of the instantaneous wind speed. It revealed more occurrences of the instantaneous wind speed in the vicinity of the rated wind speed as the mean wind speed decreased. Previous study on the high order controller for CART, which was designed considering all of the turbine flexibilities, showed performance deterioration as the wind speed approaches the rated wind speed [5]. The speed regulation at the wind speeds close to the rated speed can be improved by gain scheduling the SDAC gains, which is not covered in this study.

Comparing the RMS and maximum speed errors, the proposed SDAC gives significant improvement with respect to the GSPI controller for the mean wind speeds higher than the linearization mean wind speed, and insignificant difference for the ones lower or equal to the linearization wind speed. Therefore, the proposed SDAC conclusively improves the speed regulation across the tested mean wind speeds. Higher turbulence intensity leads to deterioration of speed response, as shown in Fig. 9a. The SDAC results in lower generator speed error, which is an expected result because the SDAC formulation has taken into account the turbulent wind speed variation, through the process noise covariance matrix Q.

The added value of considering the flexibility of the drivetrain is the ability to regulate the drivetrain dynamic load, which comes due to the induced torsional deflections. Drivetrain load mitigation can be accomplished by adjusting the closed-loop pole locations, which

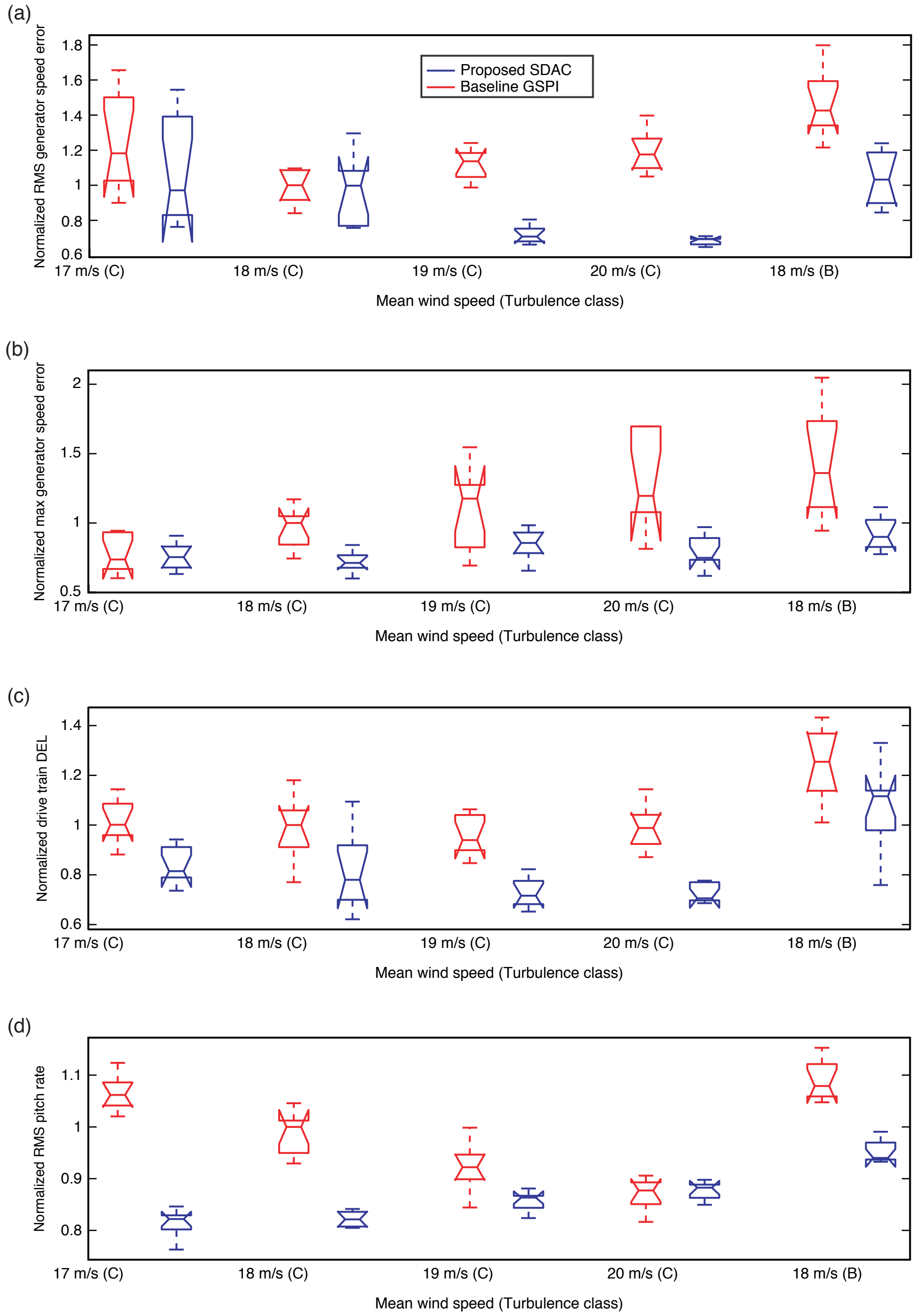

Figure 9: Performance comparisons for the NREL CART.

corresponds to the drivetrain torsional vibration. This is validated in Fig. 9d, wherein the drivetrain loads of the SDAC across different mean wind speeds and turbulence intensities are statistically lower than those of the GSPI controller, which does not take into account the flexibility of the drivetrain.

For CART, the achievement of better speed regulation and lower drivetrain load of the SDAC generally come with a statistically lower control cost (i.e. lower pitch rate) than that of the GSPI controller, as shown in Fig. 9c. For the mean wind speeds lower than or equal to 19 m/s, as well as for the higher turbulence intensity, the control cost of the GSPI is significantly higher due to the implementation of the integral anti windup. At low mean wind speeds and/or high turbulence intensities, the instantaneous wind speed more often interchanges between Regions 2 and 3. This region transition, combined with the low inertia of the turbine, contributes to high fluctuations in the rotational speed and forces the pitching actuation to saturate at its maximum rate of 18°/s.

4.2.2. NREL 5-MW Reference Turbine

As shown in Fig. 10, the general trends observed for the CART in terms of the speed regulation and drivetrain load also prevail in the case of NREL 5-MW Turbine. Therefore, these two case

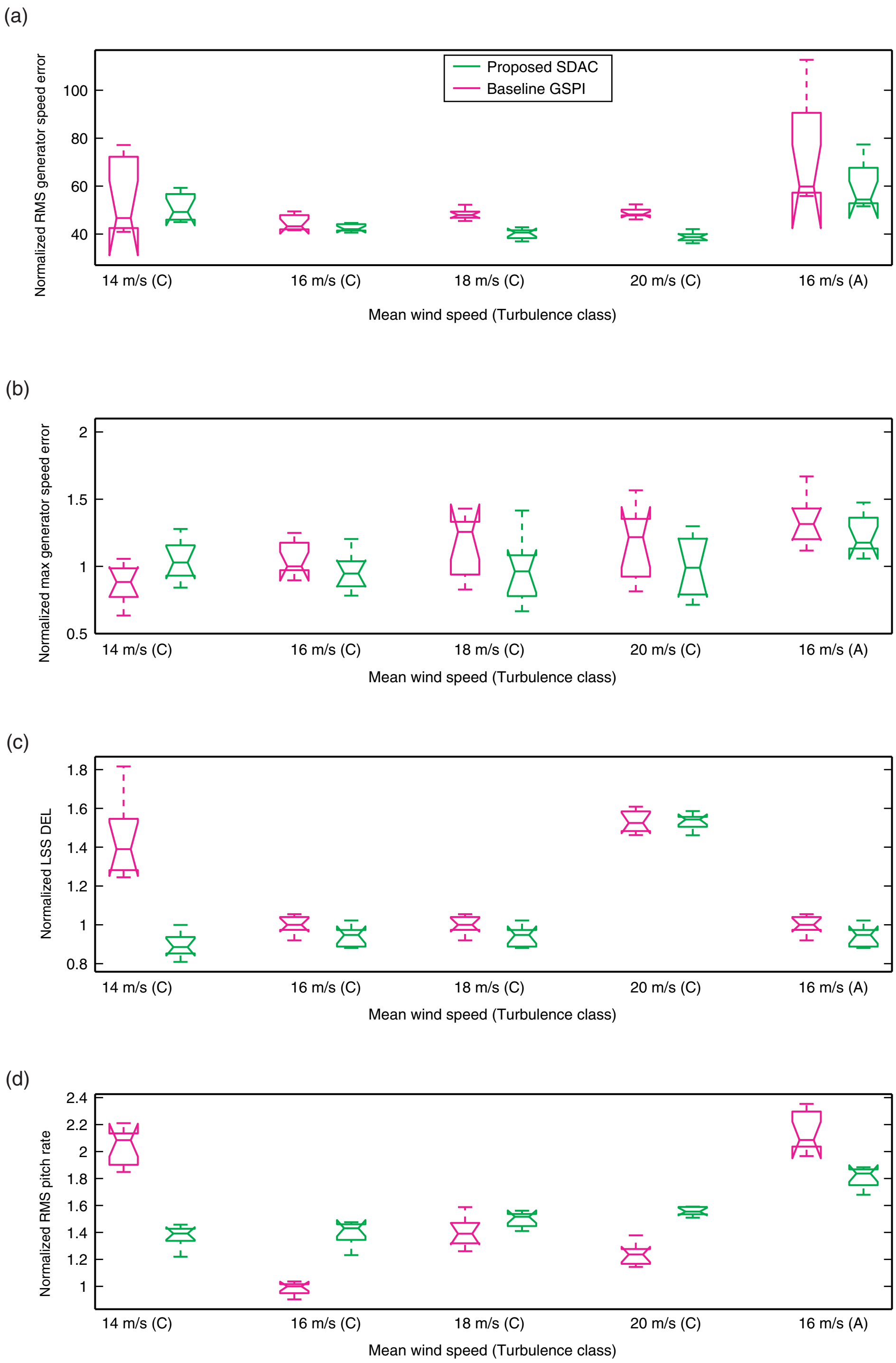

Figure 10: Performance comparisons for the NREL 5-MW reference turbine.

studies, which aim to explore the opposite ends on the rated power range of the modern utility scale wind turbines, provides confidence in the performance of the proposed controller. However, for this turbine, better speed regulation and lower drivetrain load are generally obtained with higher control cost of SDAC than that of GSPI controller, as shown in Fig. 10d. This distinction is due to the higher inertia of the turbine, which reduces the speed fluctuation and remedies the integral anti windup problems of the GSPI controller. The additional control objective of SDAC to reduce the drivetrain load dominates the total control cost, which in turn is higher than that of the GSPI controller. However, the predominant control cost due to the implementation of the integral anti windup in the GSPI controller is still visible at the lowest tested mean wind speed and higher turbulence intensity.

5. CONCLUSIONS

Previous studies have highlighted the undesirable and destabilizing effects of the unmodeled higher order structural dynamics on the design of Disturbance Accomodating Control (DAC) for wind turbine applications. This paper proposes the use of Kalman estimator in designing the Stochastic Disturbance Accommodating Control (SDAC) scheme to stabilize the system with unmodeled dynamics (i.e. higher structural flexibility). In order to investigate a general performance of the proposed control scheme, simulations have been performed on two different wind turbine configurations under turbulent wind conditions with various mean speeds and turbulence intensities. The turbines represent the lower and higher ranges of the utility scale wind turbines. The presented SDAC is able to achieve better speed regulation and lower drivetrain load under the tested wind conditions for both turbine configurations. Contrary to the general expectations, the presented SDAC utilizes lower pitch rate for simulations on the smaller wind turbine, despite the additional control objective of dampening the drivetrain load. The observed reduction in control cost of SDAC is a combined result of the nature of the turbulent wind speed and implementation of the integral anti windup in the GSPI controller.

ACKNOWLEDGEMENT

The authors would like to acknowledge the financial support from the Energy Innovation Programme Office of Singapore and the Energy Research Institute at Nanyang Technological University (ERI@N). The authors would also like to acknowledge the US National Renewable Energy Laboratory (NREL) for making FAST and MLife codes available to the public.

REFERENCES

[1] E. A. Bossanyi. Wind turbine control for load reduction. *Wind Energy,* 6(3):229–244, 2003.

[2] E. L. van der Hooft, P. Schaak, and T. G. van Engelen. *Wind turbine control algorithms.* Technical Report ECN-C-03-111, The Energy Research Center of the Netherlands, 2003.

[3] C. D. Johnson. Theory of disturbance accommodating controllers. *Leondes, C.T., ed. Control and Dynamic Systems; Advances Theory and Applications,* 12:387–489, 1976.

[4] C. D. Johnson. Disturbance-accommodating control; an overview. In *American Control Conference,* pages 526-536, Seattle, Washington, 1986.

[5] A. D. Wright. *Modern Control Design for Flexible Wind Turbines.* PhD thesis, University of Colorado at Boulder, 2004.

[6] A. D. Wright, L. J. Fingersh, and K. A. Stol. Testing controls to mitigate fatigue loads in the controls advanced research turbine. In *17th Mediterranean Conference on Control and Automation,* pages 1275–1282, Thessaloniki, Greece, 2009.

[7] K. Stol and M. J. Balas. Periodic disturbance accommodating control for speed regulation of wind turbines. In *Proceedings of AIAA/ASME Wind Energy Symposium,* pages 310-320, Reno, Nevada, 2002.

[8] M. Balas, Y. J. Lee, and L. Kendall. Disturbance tracking control theory with application to horizontal axis wind turbine. In *Proceedings of AIAA/ASME Wind Energy Symposium,* pages 95–99, Reno, Nevada, 1998.

[9] S. A. Frost, M. J. Balas, and A. D. Wright. Direct adaptive control of a utility-scale wind turbine for speed regulation. *International Journal of Robust and Nonlinear Control,* 19(1):59–71, 2009.

[10] M. M. Hand and M. J. Balas. Blade load mitigation control design for a wind turbine operating in the path of vortices. *Wind Energy,* 10(4):339–355, 2007.

[11] A. D. Wright and P. Fleming. Refinements and tests of an advanced controller to mitigate fatigue loads in the controls advanced research turbine. In *Proceedings of the 49th AIAA Aerospace Sciences Meeting,* Orlando, Florida, 2011.

[12] I. P. Girsang and J. S. Dhupia. Performance of linear control methods for wind turbines dealing with unmodeled structural modes. In *ASME Dynamic Systems and Control Conference,* Fort Lauderdale, Florida, 2012.

[13] J. George, P. Singla, and J. Crassidis. Stochastic disturbance accommodating control using a kalman estimator. In *AIAA Guidance, Navigation and Control Conference and Exhibit,* Honolulu, Hawaii, 2008.

[14] K. A. Stol. *Geometry and Structural Properties for the Controls Advanced Research Turbine (CART) for Model Tuning.* Subcontractor Report NREL/SR-500-32087, The National Renewable Energy Laboratory, Golden, Colorado, 2004.

[15] J. Jonkman, S. Butterfield, W. Musial, and G. Scott. *Definition of a 5-MW Reference Wind Turbine for Offshore System Development.* Technical Report NREL/TP-500-38060, The National Renewable Energy Laboratory, Golden, Colorado, 2009.

[16] J. H. Laks, L. Y. Pao, and A. D. Wright. Control of wind turbines: Past, present, and future. In *American Control Conference,* pages 2096–2103, 2009.

[17] J. H. Laks, L. Y. Pao, A. D. Wright, N. Kelley, and B. Jonkman. The use of preview wind measurements for blade pitch control. *Mechatronics,* 21(4):668 - 681, 2011.

[18] Herbert E. Merritt. *Hydraulic Control Systems.* Wiley, New York, 1967.

[19] P. F. Odgaard, J. Stoustrup, and M. Kinnaert. Fault tolerant control of wind turbines a benchmark model. In *Proceedings of the 7th IFAC Symposium on Fault Detection, Supervision and Safety of Technical Processes,* pages 155–160, Barcelona, Spain, 2009. IFAC.

[20] F. Dunne, L. Y. Pao, A. D. Wright, B. Jonkman, and N. Kelley. Adding feedforward blade pitch control to standard feedback controllers for load mitigation in wind turbines. *Mechatronics,* 21(4):682–690, 2011.

[21] D. Schlipf, L.Y. Pao, and P. W. Cheng. Comparison of feedforward and model predictive control of wind turbines using lidar. In *2012 IEEE 51st Annual Conference on Decision and Control,* pages 3050–3055, 2012.

[22] J. M. Jonkman. *Dynamics Modeling and Loads Analysis of an Offshore Floating Wind Turbine.* PhD thesis, University of Colorado at Boulder, 2007.

[23] IEC 61400-12. *Wind turbine generator systems - Part 12: Wind turbine power performance testing.* International Electrotechnical Commision, Geneva, Switzerland, first edition, 1996.

[24] B. J. Jonkman. *TurbSim Users Guide: Version 1.50.* Technical Report NREL/TP-500-46198, The National Renewable Energy Laboratory, Golden, Colorado, 2009.

[25] IEC 61400-1. *Wind turbines Part 1: Design requirements.* International Electrotechnical Commision, Geneva, Switzerland, third edition, 2005.

[26] G. J. Hayman and M. L. Buhl Jr. *MLife Users Guide for Version 1.00.* Technical report, The National Renewable Energy Laboratory, Golden, Colorado, 2012.

[27] B. Hahn, M. Durstewitz, and K. Rohrig. *Reliability of Wind Turbines.* Technical report, Institut fur Solareenergieversorgungstechnik (ISET), Verein an der Universitat Kassel, Kas- sel, Germany, 2006.

[28] P. Asmus and M. Seitzler. The wind energy operation & maintenance report. *Wind Energy Update,* February 2010.